Eidgenössische Technische Hochschule Zürich
Swiss Federal Institute of Technology Zurich

Semester thesis

Mechanically Controllable Break-Junctions

Presented by:	Silvan Burch
Supervisor:	Gabriel Puebla
Handed-in to:	Prof. Dr. Andreas Wallraff,
	Laboratory for Solid State Physics, ETH Zürich

Zürich, July 2008

Abstract

The development of a method to create nanometer spaced electrodes by mechanically breaking nanowires in a controlled way is presented. These mechanically controlled break-junctions (MCBJ) were fabricated as freestanding gold wires on a silicon substrate and were subsequently thinned by electromigration. Then, by using a self-constructed holder and a micrometer screw, we applied a force to these junctions by bending the substrate, creating controllable nanometer spaced electrodes. A well controlled breaking and subsequent characterization of the MCBJ by measuring the tunnel current proved to be unfeasible in the implemented prototype setup.

Contents

1 Introduction **1**

2 Theory **2**
2.1 Mechanically controllable electrodes 2
2.2 Electromigration 3
2.2.1 Quantized conductance 4
2.2.2 Breaking phases of the electromigration process 5
2.3 Tunnel effect 6
2.3.1 Particle interacting with a rectangular potential barrier 6
2.3.2 Tunnel current in metal-insulator-metal (MIM) systems 7

3 Mechanical designs **9**
3.1 Precision measurement of resistances 9
3.2 Chip holder designs 10
3.2.1 Design #1 10
3.2.2 Design #2 11
3.2.3 Design #3 12
3.2.4 Design #4 13
3.3 Manufactured prototype 14

4 Measurements **15**
4.1 Substrate characterization 15
4.2 Measurement setup 16
4.3 Results 17

5 Conclusion **21**
5.1 What has been done? 21
5.2 Next steps 21

1 Introduction

It is a matter of fact, that every day new technologies are invented and it requires little time until these technologies are integrated into our everyday life. While technology is getting more complex, electronics are getting smaller and smaller. This fact is especially true for the transistor, one of the fundamental building blocks of electronic circuits. This evolution can clearly be seen in the example of PCs and laptops: While the first computers filled most of the size of a whole room, today's laptops are very light and compact.
Although many proposed limits of the minimum transistor size have been surpassed, many people are working on replacements of the conventional transistor technology, which could be miniaturized even further, for example molecular electronics. The idea of molecular electronics is to connect single molecules to electrodes creating transistors or passive electronic components. The advantages in using molecules are as follows: Molecules have a small size, they can be produced in a great number and, at molecular scales, even quantum effects could be utilized. Furthermore the molecular structure defines the electrical properties of the molecules. Hence, the electrical behavior of a molecule can be specifically tailored to the task at hand using molecular design and synthesis [1]. The first step towards molecular electronics is the creation of nanometer spaced electrodes which will contact the molecules.
The topic of this semester thesis is the implementation of mechanically controllable break-junctions which are one way to create these nanometer spaced electrodes. Break-junctions are thin sections of wire which are broken in such a way that a very small gap is formed. In our case we want to break a gold nanowire by applying a force to the substrate on which this wire is deposited. This force will bend the substrate, which is held by two counter supports, applying a strain to the junctions. After breaking the junctions mechanically, the size of the gap between the electrodes should be tunable in the Angstrom range due to reduced translation between vertical movement and electrode spacing. By measuring the tunnel current between the electrodes, it should be possible to measure the distance between the electrodes. This method is employed by several groups working on molecular electronics.
The theory of mechanically controllable electrodes, electromigration and tunneling currents will be discussed in chapter 2, where the necessary knowledge for this semester thesis will be given. In chapter 3, some possible designs for a substrate holder will be shown and discussed as well as the manufactured prototype holder. Finally, the measurement setup and the results will be presented in chapter 4.

2 Theory

In this chapter we will discuss the theoretical background of this semester thesis. It will cover how to mechanically control the separation of two electrodes on a sub Angstrom scale, as well as an introduction to electromigration and the tunnel effect.

2.1 Mechanically controllable electrodes

While tunable nanometer spaced electrodes can easily be achieved with a Scanning Tunneling Microscope (STM), this method requires a complex setup and is not optimal in terms of mechanical stability. A simpler approach is the use of a flexible substrate to attenuate a coarse mechanical drive to sub nanometer electrode spacing. Figure 2.1 shows a schematic of the experimental setup. The substrate is held by two counter supports while a force is applied to the chip by a push-rod, in our case a micrometer screw. When the substrate is bent, the top surface is increased, which in turn separates the freestanding electrodes.

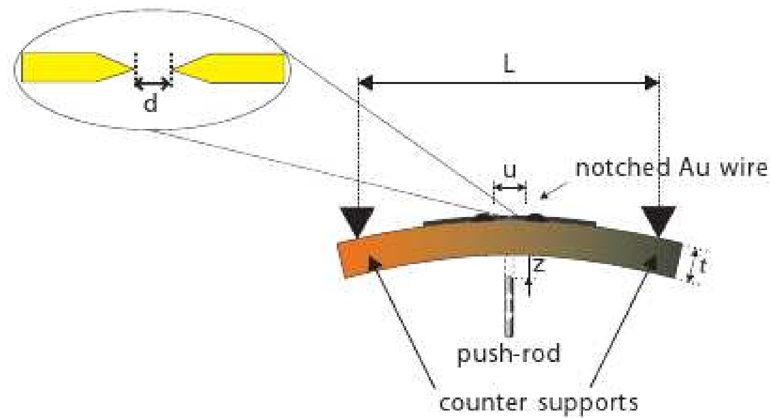

Figure 2.1: Bending a silicon chip with two counter supports [2].

First, we want to find out how the gap d increases as we bend the chip by some z. We assume that the bending is elastic and d is proportional to z:

$$d := a \cdot z, \tag{2.1}$$

where a is the so called attenuation factor. The attenuation factor can be calculated geometrically using elastic beam theory. Assuming a beam with supported ends, we can calculate the geometrical attenuation factor a_g using the following equation [2]:

$$a_g = \frac{6ut}{L^2}, \tag{2.2}$$

where u is the suspended section of the junction, t the thickness of the substrate and L the length of the chip between the two counter supports. Our chips have the following dimensions: $u \approx 300$ nm, $t = 500$ μm and $L \approx 1$ cm. This results in an attenuation factor of

$$a_g \approx 9 \cdot 10^{-6}, \tag{2.3}$$

which means that moving the micrometer screw by 10 μm corresponds to a change of about 1 Å in gap size. Further, if we know how much we can bend the silicon chip, we can calculate the equivalent force by applying the following formula [3]:

$$F = \frac{48EI_x}{L^3} z \tag{2.4}$$

where z is the bending distance, E is Young's Modulus and I_x is the area moment of inertia. For silicon, we can take Young's Modulus as $E = 150$ GPa and we can use the following equation for the area moment of inertia [4]:

$$I_x = \frac{bt^3}{12} \tag{2.5}$$

where t is the thickness of the chip and b the width. We can also calculate the chip's increase of length of surface due to the force applied by the rod using following equation:

$$L + \Delta L = 2 \int_0^{\frac{L}{2}} \sqrt{1 + (\frac{FL^3}{48EI_x} \left[\frac{3}{L} - \frac{12z^2}{L^3} \right])^2} dz. \tag{2.6}$$

2.2 Electromigration

The substrate of choice for conventional microfabrication is silicon, which is, unfortunately, not very flexible and restricts the maximum bending. To compensate for this restriction, the break-junction must be made very thin, optimally already on the order of tens of atoms in cross-section. As this size scale is inaccessible by lithography, we need to 'prethin' the junctions. One of the leading causes of failure in electronic devices are open or shorted lines due the current driven mass flow in conductors. This effect occurs at high current densities and is called electromigration. It can be utilized to create the required wire cross-sections.
How does electromigration work? Metals are lattice structures, which are created due to repulsion and binding forces of the metal ions. These ions are oscillating within the lattice. If an electrical current is applied to a metal, electrons will flow through and scatter at the ions, thereby transferring energy and momentum. As soon as an ion gets

enough energy, it is possible for this ion to flow away from its position within the lattice structure. The mass flux J_m within the metal can be described by the following expression:

$$J_m = -L^*_{m,m}(\nabla\mu^m - (Z - \frac{L_{m,e}}{L_{m,m}})e\rho j) \tag{2.7}$$

where Z is the ion charge, $L_{m,*}$ are constants proportional to the diffusion coefficient, $L^* = \frac{L}{T}$ with the temperature T, the $\mu's$ are the chemical potentials related to electrons (^{e}) and ions (^{m}) and $Z^* = (Z - \frac{L_{m,e}}{L_{m,m}})$ is the effective charge. Normally, Z^* is positive, which means the net force will be in opposite direction to the electric current.
We have also to take diffusion effects into account, therefore we introduce the diffusion coefficient D, which describes the mobility of particles:

$$D = D_0 e^{(\frac{-E_A}{kT})} \tag{2.8}$$

where E_A is the activation energy, as only atoms with enough energy need to be taken into account. As we can see, D depends strongly on the temperature.
If we had a perfect lattice, we would see almost no diffusion effects due to the lattice symmetry. Our gold wires consists of small regions of perfect crystal structure. These crystal pieces have different orientation and therefore, the symmetry is broken. At these grain boundaries, the ions are less bound than at other points in the material, hence the activation energy for them is smaller. It is at these points where the diffusion effects take place.
Furthermore we have to take Joule heating into account, which is heat generated by the scattering of electrons on the metal ions. This heating occurs mostly at the already mentioned grain boundaries, because the electrons will scatter more at these points. The activation energy for the ions at these points is smaller, too. The local temperature will lead to an increase of diffusion and migration effects. These will result in an other increase of Joule heating, creating a vicious cycle. If electromigration is not controlled, Joule heating will melt a gap into the metal wire.

2.2.1 Quantized conductance

If the cross section of the nanowire reaches the size of the Fermi wave length of electrons during electromigration, the conductance will no longer drop continuously but in a quantized fashion. We will look at a simple model to explain this behavior.
We replace the continuous current by a discrete number of electrons flowing, which yields the following equation:

$$I = \frac{\Delta Q}{\Delta t} = \frac{\Delta N e}{\Delta t} = \Delta N e \frac{v}{L} \tag{2.9}$$

with the elementary charge e, the distance covered by the electrons L and the number of electrons ΔN passing through the wire within the time Δt. Using Ohm's law we get

$$G = \frac{I}{V} = \frac{\Delta Nev}{LV}. \tag{2.10}$$

To take quantum mechanics into account, we introduce the de Broglie wave length of a particle in a box as $\lambda = \frac{L}{n}$ with $n \in \mathbb{N}$. Furthermore, we use the Heisenberg Uncertainty Principle $\Delta p \Delta x \leq h$ (with h the Planck constant) and the momentum given by $p = mv$ to reach

$$mv\frac{L}{n} \leq h. \tag{2.11}$$

According to Pauli, no two electrons can be in the same quantum state. If we consider the spin degeneracy, we get the relation $2n = \Delta N$. By inserting this in (2.11), we get

$$\Delta N = \frac{2Lm\Delta v}{h}. \tag{2.12}$$

We rewrite the change in potential energy as $\Delta U = eV$, which is equal to a change in kinetic energy $\Delta T = mv\Delta v$. Using this relation and equations (2.10) & (2.12), we find

$$G = \frac{2e^2}{h} \equiv G_0. \tag{2.13}$$

Here $G_0 = 7.75 \cdot 10^{-5}$ S is the conductance quantum, which gives the possible values for quantized conductance if multiplied by $n \in \mathbb{N}$. This follows from the Landau Formalism [5] which provides a more general description of a current flowing through narrow constrictions taking into account the width of the conductor. The electrons in the junctions form a typical particle in a box problem of elementary quantum mechanics. Solving the Schrodinger equation for this setup shows that there is a discrete number of eigenstates for this system and the total energy consists of the sum of these energy modes. In the case of break-junctions, it can be assumed that a conductance unit of 1 G_0 is assigned to every of these eigenstates. It can now be seen why the possible values for the quantized conductance are a multiple of G_0.

2.2.2 Breaking phases of the electromigration process

At the beginning of the electromigration process, the nanowire is a normal contact with diffusive electron transport. Voltage and current increase linearly up to the point where electromigration sets in. The electromigration will reduce the cross section of the wire and at a conductance of about 20 G_0, the wire will reach the size of the Fermi wave length where quantum effects will appear. The conductance will drop in a quantized way down to 1 G_0, at which point we have a single atom (quantum point contact) or a chain of atoms between the electrodes. Migrating beyond this point will break the wire, after which only tunneling is possible (see figure 2.2).

We would like to utilize electromigration to thin the break junction to a point where the limited bending of the silicon substrate is enough to break the nanowire.
For a more in depth discussion of electromigration, see [6].

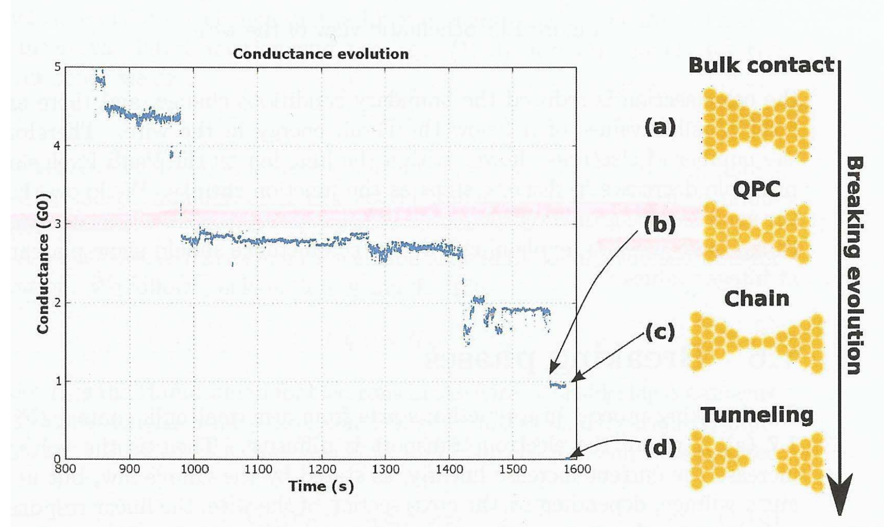

Figure 2.2: (a): The electron transport is diffusive at about 20 G_0. (b) and (c): The conductance is around 1 G_0 for a quantum point contact and a chain of atoms. (d): We have a very small conductance for a tunnel current.

2.3 Tunnel effect

As the separation of the electrodes is beyond the resolution of most microscopes, we need some other method to measure the gap size. This is done by measuring the tunnel current, which will give us information about the size of the gap between the electrodes. Classically, it is impossible for a particle to pass a potential barrier if the potential height is bigger than the total energy of the particle. The tunnel effect is a quantum mechanical effect which predicts that even if the total energy of the particle is smaller than the potential height, there is a possibility for the particle to pass the barrier.

2.3.1 Particle interacting with a rectangular potential barrier

To understand the tunnel effect, we have to consider the wave aspects of a single particle. The wave function describing the particle, $\Psi(\vec{x},t) = \psi(\vec{x})\chi(t)$, is a solution to the Schrodinger equation and $|\Psi|^2 d^3x$ is the probability to find the particle in the volume element d^3x. We now consider the one dimensional problem of a rectangular potential barrier with the following properties:

$$U(x) = \begin{cases} 0 & x < 0 \\ U_0 & 0 \leq x \leq L \\ 0 & x > L. \end{cases} \tag{2.14}$$

We are interested in solutions $\psi(x)$ of the stationary Schrodinger equation

$$\Big(-\frac{\hbar^2}{2m}\frac{\partial^2}{\partial x^2} + U(x) \Big)\psi(x) = E\psi(x). \tag{2.15}$$

Assuming the particle comes from $-\infty$ and goes to ∞, we find

$$\begin{aligned} \psi(x) &= e^{ikx} + re^{-ikx} && x < 0 \\ \psi(x) &= Ae^{ilx} + Be^{-ilx} && 0 \leq x \leq L \\ \psi(x) &= te^{ikx} && x > L \end{aligned} \tag{2.16}$$

with $k = \frac{\sqrt{2mE}}{\hbar}$ and $l = \frac{\sqrt{2m(E-U_0)}}{\hbar}$. The constants r, A, B and t are determined by the continuity condition. As we can see, l is imaginary because $E - U_0 < 0$. The transmission probability is defined as $T = |t|^2$ and is given by

$$T = |t|^2 = \left(1 + \frac{\sinh(2|l|L)U_0^2}{4E(U_0 - E)}\right)^{-1}. \tag{2.17}$$

For a classical particle the region $x > L$ is not accessible but for a quantum mechanical particle the transmission probability is $T \neq 0$. Furthermore, we can see that T falls off exponentially with L and $(U_0 - E)$ [7, 8].

2.3.2 Tunnel current in metal-insulator-metal (MIM) systems

If we consider the tunnel current through an insulator between two metal electrodes (MIM system), the John G. Simmons formula [9] allows the derivation of an expression for the tunnel current. This situation is shown in figure 2.3 and is analog to our situation.

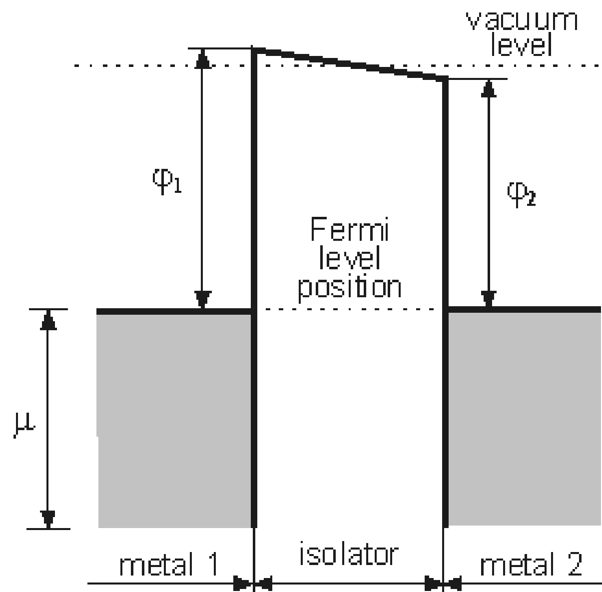

Figure 2.3: Diagram of a MIM system in equilibrium.

The two metal electrodes are separated by an insulator of thickness L. We can use the following equations to describe the tunnel current:

$$J = \frac{\gamma\sqrt{\bar{\phi}}V}{\delta_z} e^{-A\delta_z\sqrt{\bar{\phi}}} \tag{2.18}$$

$$\gamma = \frac{e\sqrt{2m}}{4\beta\pi^2\hbar^2} \tag{2.19}$$

$$\beta = 1 - \frac{1}{8\bar{f}^2\delta_z}\int_{z_1}^{z_2}\left[f(z) - \bar{f}\right]^2 dz \tag{2.20}$$

where $\delta_z = L$ is the barrier width, $\bar{\phi} = \frac{\phi_1+\phi_2}{2}$ is the average barrier height, V is the voltage between the electrodes and $A = 2\beta\sqrt{\frac{2m}{\hbar^2}}$. The functions $f(z)$ and $\bar{f}$ are given by the shape of the potential. In our case, we have

$$f(z) = \tfrac{\phi_2-\phi_1}{\delta_z}z + \phi_1 \approx \phi_1 \quad and \quad \bar{f} = \tfrac{1}{\delta_z}\textstyle\int_{z_1}^{z_2} f(z)dz. \tag{2.21}$$

We can assume $f(z) \approx \phi_1$ because in our case $\phi_1 \approx \phi_2$ as we set the voltage as we measure. Furthermore, $\bar{\phi} >> 1eV$, so we can consider $\bar{\phi}$ to be independent of the voltage V.

3 Mechanical designs

To allow a controlled mechanical breaking of a nanowire, one of the essential experimental components is a sample holder. This holder needs to fulfill several requirements, such as making mechanical points available against which the chip can be pressed, creating contacts to the wire on the bridge and also a simple way to mount the chip. To fulfill these requirements, several design approaches are possible. In the following sections, some ideas for contacting and mounting are suggested, as well as a review of the prototype mounting which was used for different measurements.

3.1 Precision measurement of resistances

In a typical two point resistance measurement, the electrodes contribute to the measured resistance of the device, thus introducing a systematic error. To avoid this problem, we separate the voltage measurement from the current measurement. This is called a four point measurement or four-terminal sensing. Since there is no current flowing through the voltmeter electrodes we have no voltage drop in the lead and we acquire more precise results due to eliminating the impedance contribution of the wiring and the contact resistances [4]. The measurement scheme is shown in figure 3.1 [10].

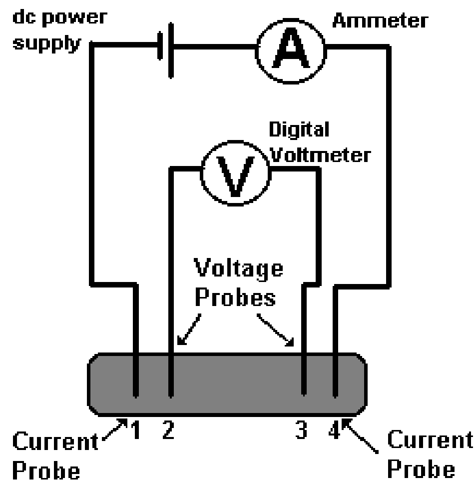

Figure 3.1: Scheme of a four-terminal sensing measurement.

3.2 Chip holder designs

Depending on the requirements, different chip holder designs can be thought of, where the main challenge is establishing electrical contact between the chip and the holder. In this section some possible designs are presented along with their advantages, disadvantages and contacting possibilities.

3.2.1 Design #1

A simple U-design is shown in figure 3.2. The chip lies on the edges and is pushed by a rod (in our case a micrometer screw) against the two bars. With this mounting, it is easy to mount the chip by hand because there is some free space, making it possible to adjust the chip to provide contact.
One possible scheme for contacting is the use of copper wire or thin copper strips at four points around the two bars (in this case insulating, see figure 3.3). As soon as the micrometer screw pushes the chip against the bars, the four points create an electrical connection. A further possibility would be cutting the bars in half and making them out of copper, so that the bars themselves would be the contacts, although this necessitates an insulation between the rods and holder.

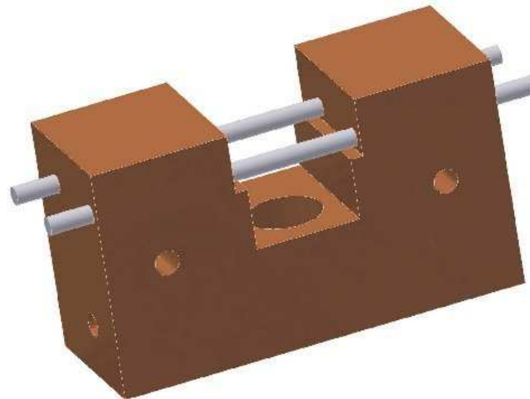

Figure 3.2: Design #1: A simple U.

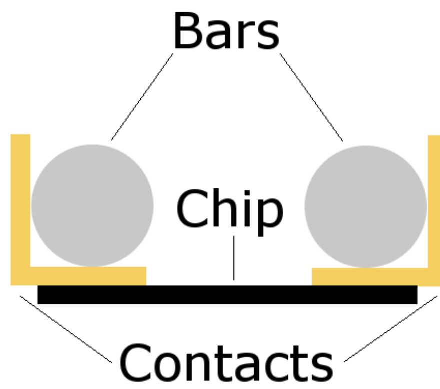

Figure 3.3: Contacting with copper strips.

3.2.2 Design #2

This design is a variation of the first one. An attachment is made as shown in figure 3.4 in which we can mount the chip. Thus the whole mounting is divided in two separate parts: the U-part holding the micrometer screw and a second part to hold the chip. This separation makes it easier to deal with mounting the chip in the holder because one can remove the little part from the whole mounting. Unfortunately, this separation can also be a bit problematic because of fixing and releasing the attachment from the U-part. During this process, a displacement of the mounted chip can easily occur.
The possibilities for contacting are the same as with design #1.

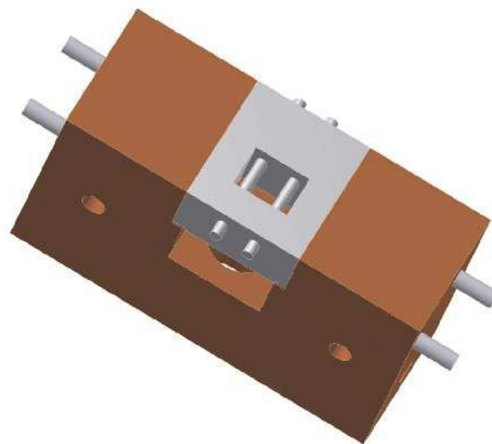

Figure 3.4: Scheme of design #2.

3.2.3 Design #3

A simplified design is shown in figure 3.5. It is easy to mount the chip into the holder because one can move the chip freely. On the other hand it is not so easy to correct the position of the chip within the mounting because the chip is only held by the micrometer screw and not by a frame.
There are several options for creating a contacting here. Assuming the mounting is made out of an insulator to avoid unintentional contacting, copper wires or strips could be placed analog to the previous contacting ideas. Alternatively, we could make the poles out of three layers: a conducting layer, an insulating layer and a conducting layer, thus the conducting layers are the contacts as shown in figure 3.6. Another idea would be to drill four holes through the poles and to put a conducting spring through each hole. Thus we get a contact as soon as we press the chip against the poles using the springs for flexibility.

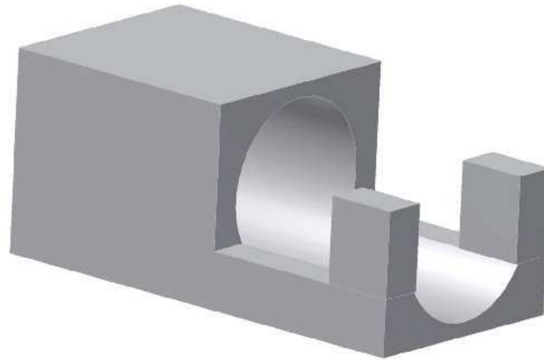

Figure 3.5: Scheme of design #3.

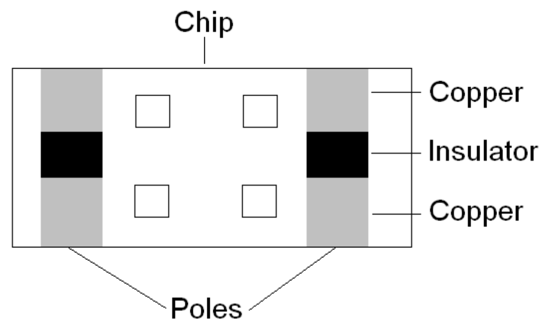

Figure 3.6: Contacting with three-layer poles.

3.2.4 Design #4

Figure 3.7 is the most interesting design. In principle, it is the same design as #1 but cut into four pieces in such a way that every piece of the mounting is also part of the contacting, the biggest advantage of this design. A disadvantage is that manufacturing this mounting could prove to be difficult. One possible way to assemble this holder would be to put a layer of insulator between the parts and fix the whole mounting on a plate.

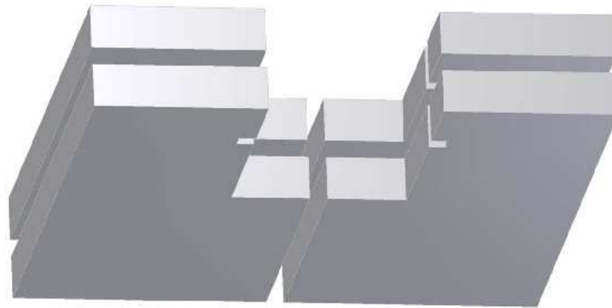

Figure 3.7: Scheme of design #4.

3.3 Manufactured prototype

The implemented mounting is similar to design #2 (figure 3.4). This design was chosen because of ease of construction. Furthermore, all the materials necessary were immediately available. The U-part was made out of copper, the attachment and the two bars for holding the chip out of plexiglass. In addition, a little steel orb was put on our micrometer screw, so the force acted on a certain point on our chip. For contacting, little copper strips were made and glued onto four points of the attachment. Figures 3.8 & 3.9 show the manufactured prototype.

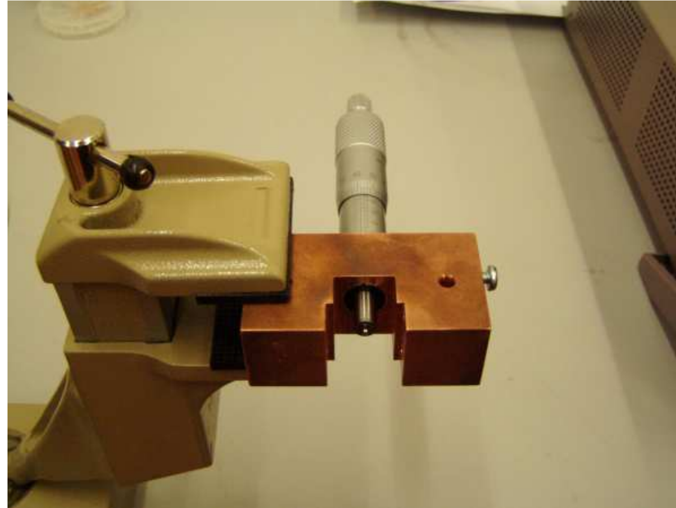

Figure 3.8: Manufactured prototype.

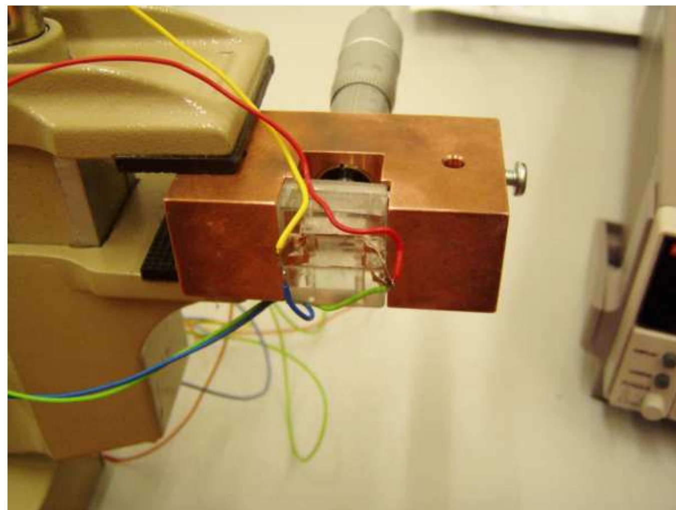

Figure 3.9: Manufactured prototype inclusive attachment.

4 Measurements

We have seen what mechanically controlled break-junctions are and how we can use electromigration for our purpose. In this chapter, we will take a look at the substrate characterization and the results of our measurements with the break-junctions.
In figure 4.1, we can see the layout of a typical silicon chip similar to the ones we used for measurement. The dimensions are 6 mm by 6 mm. The four sites (A,B,C,D) provide contact for the four point measurement of 4 junctions each. The pattern on the surface of the silicon chip is created in two steps: one step of conventional photo lithography for the bond pads and one step of electron beam lithography to define the gold nanowires.

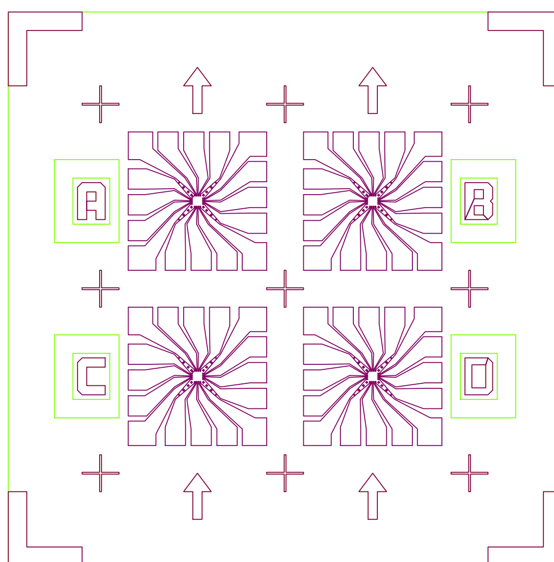

Figure 4.1: Design of a silicon chip.

4.1 Substrate characterization

In order to get a fully working MCBJ, we first had to characterize the properties of the silicon substrate. To this end, silicon pieces were mounted in the prototype sample holder and the displacement necessary to break them was measured. The experimental protocol was as follows: first, the substrate was mounted into the holder. Then, a laser pointer was deflected off the pieces. A change in the diffraction pattern of the laser beam indicated that the micrometer screw was applying a force, thus allowing the definition of a zero point. Finally, the micrometer screw was turned until the chip broke.

The breaking forces of several silicon pieces are listed in table 4.1. Note that this force is different for every piece because the pieces were not all exactly equal. If we use (2.6) with the results from table 4.1, we get an idea of how much the surface of the silicon chips increase during the bending process (see table 4.2).
These results show us that the bending is good enough to help creating mechanically controllable break-junctions as the elongation over the whole surface corresponds to an elongation of the gap size of about nm size.

Piece	Dimension $x \cdot y$, $[mm^2]$	Bending z, $[mm]$	Force F, $[N]$
1	$12 \cdot 6$	0.265	8.63
2	$12 \cdot 5$	0.140	3.80
3	$13 \cdot 6$	0.080	2.05
4	$12 \cdot 5$	0.105	2.85
5	$10 \cdot 5$	0.165	7.73
6	$9 \cdot 5$	0.205	13.18
7	$10 \cdot 5$	0.275	12.89

Table 4.1: Breaking forces of different silicon pieces with different dimensions. Note that the pieces were not all of exact the same shape although some were of about the same size.

Piece	Length of surface bending ΔL, $[\mu m]$	Expected electrode spacing d, $[nm]$
1	14.03	2.39
2	3.92	1.26
3	1.18	0.72
4	2.20	0.95
5	6.53	1.49
6	11.20	1.85
7	18.13	2.48

Table 4.2: Increase of surface of a silicon piece due to bending with a rod and the expected electrode spacing calculated using the attenuation factor $a_g = 9 \cdot 10^{-6}$ derived in section 2.1.

4.2 Measurement setup

After determining that, in principle, it should be possible to create a mechanically controllable break-junction using gold wires on a silicon substrate, first attempts to implement this were done. The measurement setup consisted of the setup for breaking silicon pieces, i.e. the prototype sample holder, a laser pointer and adding a 'Keithley 2600' source measure unit (SMU) to electromigrate the sample and for measuring tunnel currents (see figure 4.2). To perform a four-point measurement four sensing wires leading to

the probe are necessary. We can see in figure 4.3 that every junctions has four contacts for this purpose. To achieve contact on a standard electromigration chip (6 mm · 12 mm), we did the following: The four outer squares were used as contacts by bonding the whole area together (indicated by the red lines on figure 4.3). Then, each of these contacts was connected to one of the four contacts of the junction. Subsequently the SMU was connected to these contacts by using the copper strip-contacting scheme seen in section 3.2 (figure 3.3).
Electromigration was done using a feedback control program developed for electromigrated break-junctions (EMBJ) [6].

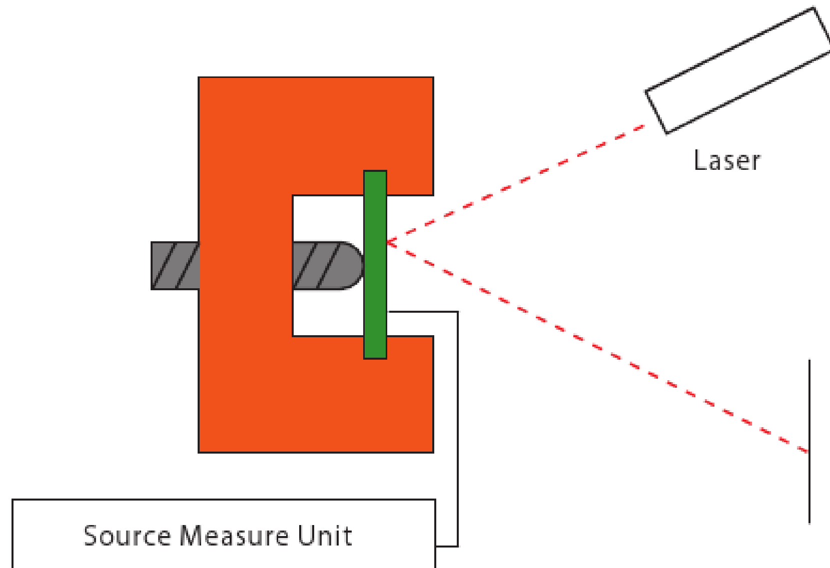

Figure 4.2: Measurement setup.

4.3 Results

The goal of this semester thesis was to control the breaking of a gold nanowire using a mechanical force. During this procedure, we faced different problems. First, it took us some time to figure out how to mount the chip into the holder and how to connect the SMU to the junctions without destroying them. The problem was that the SMU overcharged the junctions when we started it. This problem was resolved by short-circuiting the wiring during the initialization phase of the SMU. Further, we grounded everything that came into contact with the sample holder or the sample itself to minimize the danger of electrostatically destroying the junction.
After solving this problem, the junctions still broke before or during the electromigration process. We found the reason for that in the laser pointer which was used to define a zero point for the micrometer screw. Although it was a weak laser, it obviously had enough power to become a problem. Many junctions were destroyed due to possible

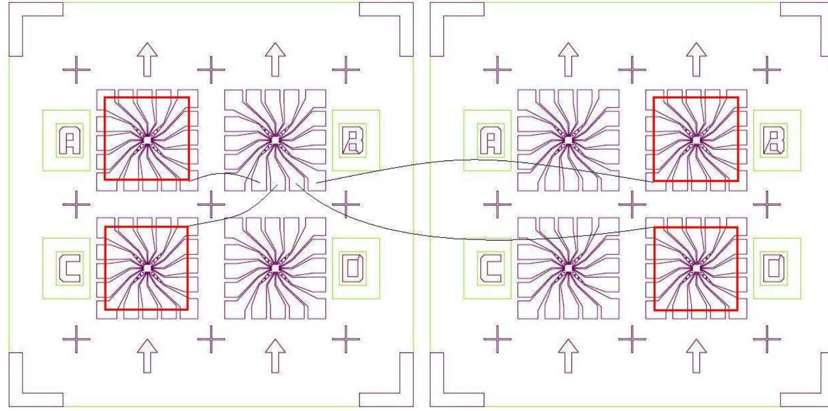

Figure 4.3: Mask outline of a typical silicon chip. The black lines indicate the four contacts of a junction, the red ones the contacts on the four outer squares.

electrostatic or thermal effects caused by the laser. To solve this problem we tried to point the laser at the outer areas of the chip so the junctions would not get destroyed. Later, we mounted the chip without using a laser but looking very carefully at the chip instead to find out when the micrometer screw started applying a force. Despite all this care, some chips were destroyed in the process of finding a way to mount the chip without the laser pointer.
The measurement protocol used was as follows:

1. Short-circuit the wiring.
2. Mount the chip into the holder.
3. Start the SMU (Keithley 2600).
4. Open the short-circuit.
5. Electromigrate the wire to about 3 G_0.
6. Turn the SMU off.
7. Turn micrometer screw to break the junction.
8. Record IV-curves with voltages from 1 to 100 mV and different positions of the micrometer screw.

The junction was supposed to be broken manually using the micrometer screw in order to create nanometer spaced electrodes. We tried breaking the junctions during the electomigration process at about 5 G_0 which resulted in destroyed junctions. It has been tried to stress the junctions during electromigration and breaking them when 3 G_0 were

reached as well as breaking them at 3 G_0 without prestressing. Stressing the junctions during electromigration process yielded variations of the conductance without interfering electromigration. Breaking the junctions manually was not as easy as we thought and it turned out that the micrometer screw itself was not precise enough. It was impossible to turn the screw some μm. As soon as the screw has been touched, it already moved a bit. Touching the table on which the setup was also had influence on the position of the screw. Another problem was that, after breaking the junction, we measured currents of 10^{-6} to 10^{-12} A. We could not tell whether these currents were tunnel currents or just noise as can be seen in figure 4.5. Although several measurements were made, we did not get better results. The use of unshielded wiring for the measurements is the most probable cause for the high background noise.

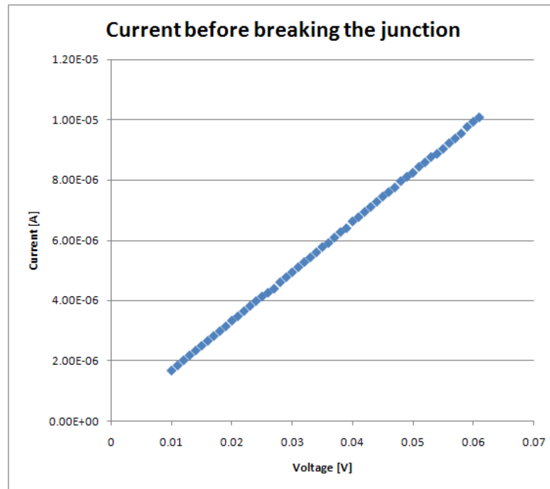

Figure 4.4: IV-curve before breaking the junction showing the expected linear behavior.

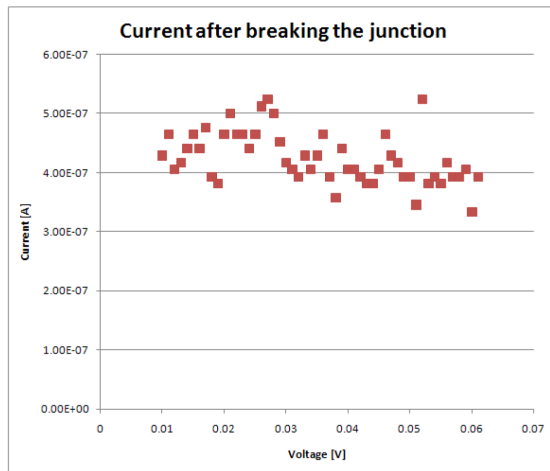

Figure 4.5: IV-curve after breaking the junction. The noise can clearly be seen in this measurement.

5 Conclusion

5.1 What has been done?

A first step towards the experimental realization of mechanically controllable break-junctions was done. A sample holder prototype was manufactured and first used to characterize the silicon substrate. It was found that silicon fulfills the requirements needed as a substrate. Later, the sample holder and a source measure unit were integrated into a measurement setup to create mechanically controllable break-junctions. The chip was mounted into the holder and was connected to a SMU. Then, the holder was fixed in a screw clamp and the gold nanowire, our break-junction, was thinned using electromigration. This step was necessary due to the small bending range of the silicon substrate. The final steps were bending the substrate with a micrometer screw and thus creating nm spaced electrodes and characterizing the mechanical control over the spacing by recording IV-curves. Measurements of the IV-curves did not yield a characterization of the mechanical properties of the break-junctions. The two main reasons for this were a very high noise level, due to unshielded wiring, and the coarse resolution of the micrometer used for bending.

5.2 Next steps

The described approach to the creation of mechanically controllable break-junctions yielded a number of possible improvements. The micrometer screw pushing against the substrate turned out not to have enough precision. A possible solution would be to replace this micrometer screw with a step motor, which would also enable computer controlled measurements. The unshielded wires and contacts used in the prototype introduced a high level of noise in the measurements. To avoid this more care needs to be invested in a satisfactory wiring scheme including, for example shielding. Finally, switching between junctions required a lot of time due to the fact that each device required its own bond run. To optimize the time management and increase comfort, the next generation of sample holder should be capable of contacting several junctions at the same time.

List of Figures

2.1 Bending a silicon chip. 2
2.2 Breaking phases of a junction. 6
2.3 Diagram of a MIM system in equilibrium. 7

3.1 Scheme of a four-terminal sensing measurement. 9
3.2 Design #1: A simple U. 10
3.3 Contacting with copper strips. 11
3.4 Scheme of design #2. 11
3.5 Scheme of design #3. 12
3.6 Contacting with three-layer poles. 13
3.7 Scheme of design #4. 13
3.8 Manufactured prototype. 14
3.9 Manufactured prototype inclusive attachment. 14

4.1 Design of a silicon chip. 15
4.2 Measurement setup. 17
4.3 Mask outline of a typical silicon chip. 18
4.4 IV-curve before breaking the junction. 20
4.5 IV-curve after breaking the junction. 20

List of Tables

4.1 Breaking forces of silicon pieces. 16
4.2 Increase of surface of silicon pieces and expected electrode spacing. 16

Bibliography

[1] FZK. Molekulare Elektronik. http://www.fzk.de/fzk/idcplg?IdcService=FZK&node=2095.

[2] Lucia Grüter. *Mechanically controllable break junction in liquid environment: a tool to measure electronic transport through single molecules.* PhD thesis, Universität Basel, 2005.

[3] ROYMECH. Elastic Bending Theory. http://www.roymech.co.uk/Useful_Tables/Beams/Beam_theory.html.

[4] Wikipedia. http://www.wikipedia.org/.

[5] Laetitia G. Soukiassian. Measuring the Conductance of Gold Atomic Wires: Quantized Conductance of a Break Junction. Work done in the group of Prof. Ron Reifenberger at Purdue University, June 2000.

[6] François Bianco. Break junctions for molecular electronics using electromigration. Semester work done in the group of Prof. Dr. Andreas Wallraff at ETHZ, 2007.

[7] NT-MDT. STM Physical Backgrounds. http://www.ntmdt.com/SPM-Techniques/Basics/1_STM/1_1_STM_Physical_Backgrounds/text153.html.

[8] Matthias R. Gaberdiel. Quantenmechanik 1. Skript zur Vorlesung, 2006/07.

[9] NT-MDT. Tunnel Current in MIM System. http://www.ntmdt.com/SPM-Techniques/Basics/1_STM/1_2_Tunnel_Current_MIM_System/text154.html.

[10] Images Scientific Instruments. http://www.imagesco.com/.